Operational Techniques for Determining SWE by Sound Propagation through Snow

NICHOLAS J. KINAR[1] AND JOHN W. POMEROY[1]

ABSTRACT

Recent research has demonstrated that an acoustic pressure wave can be used to determine snow water equivalent (SWE) without the need for gravimetric sampling. The application of this technique poses a number of challenges in cold environments due to the presence of snow with wind crusts, ice layers, buried vegetation and high liquid water content and due to the extensive signal processing required after collection of returned sound waves. To show that the technique can contribute to operational SWE surveys, portable, field-usable devices were constructed with the capability of reliable on-line signal processing and calculation of SWE in the field. Reflections of the sound wave from the snowpack were identified by a peak detector algorithm and then analyzed. The acoustic method, portable field devices and modified signal processing techniques were tested at forest and tundra sites near Whitehorse, Yukon Territory, and at forest and meadow sites in the Rocky Mountains, Alberta, Canada. Comparisons were made between the acoustic technique and gravimetric sampling conducted using snowpits and density samples of individual snow layers and with bulk gravimetric sampling using an ESC30 "snow tube" snow density sampler and ruler. These comparisons demonstrated that the acoustic measurement with the portable field unit and on-line modified signal processing technique can provide SWE estimates in the field that are of comparable accuracy to SWE calculated from gravimetric samples. The on-line processing allows the operator to gauge the reliability of the measurement and to ensure sufficient data collection before leaving the field site. Significant advantages over gravimetric sampling accrue from non-destructive sampling of the snowpack and easy of measurement. Limitations and aspects for further research are also discussed.

INTRODUCTION

Snow Water Equivalent (SWE) is the equivalent depth of water that would be available if the snowpack were transformed to liquid water (Pomeroy and Gray, 1995). The measurement of SWE is important to water resources assessments since it can be used to characterize available water from the seasonal snowcover (Pomeroy et al., 1998). Accurate assessment of water availability from snowmelt is crucial in regions where demand for water consumption exceeds the water available for use and in regions subject to snowmelt flooding. SWE has been used to determine the maximum amount of water that is potentially available as agricultural runoff during the time of ablation (Male and Gray, 1975). Measurements of SWE can also help to validate and provide inputs for atmospheric and hydrological models in respect to their accuracy over cold regions (Pomeroy et al., 2007).

Procedures used to determine SWE often involve the use of instrumentation that are time-consuming to operate, expensive to deploy, and prone to instrumental and human error. Devices which have been used in the measurement of SWE include gravimetric snow samplers; snow

[1] Centre for Hydrology, University of Saskatchewan, 117 Science Place, Saskatoon, Saskatchewan, S7N 5C8 Canada

pillows; Frequency-Modulated Continuous-Wave (FMCW) radar systems; gamma-ray attenuation and passive microwave radiation sensors (Pomeroy and Gray, 1995).

In a recent paper (Kinar and Pomeroy, 2007), a technique was presented for determining SWE by an acoustic impulse. Two sonic wave transducers were positioned above the snow surface. One of the transducers was used to send a sound wave into the snowpack. Reflections of the sound wave from the snow were captured by the other transducer and signal processing techniques were utilized to estimate SWE.

The acoustic SWE technique has a number of advantages over other SWE measurement techniques. One advantage is that the use of an acoustic wave permits non-invasive measurement of SWE. This allows for SWE measurements to be made without physically disrupting the snowpack. Changes in SWE at one location can be tracked without the need for instrumentation to be permanently installed under the snow surface. Acoustic snow surveys are logistically easier because gravimetric snow samples do not have to be extracted. Unlike radar devices, which rely on the use of high-current sourcing power supplies and large antennas to produce and receive electromagnetic waves, small and portable acoustic transducers can be powered by inexpensive electronic circuits with modest power requirements and so are suitable for remote locations and cold temperatures.

However, one disadvantage of the acoustic technique described by (Kinar and Pomeroy, 2007) is that signal processing of the sound wave reflected from the snowpack could not be performed in real-time. In a similar fashion to seismic interpretation, the signal processing performed on the sound wave generated information that must be examined by a human operator before SWE can be calculated. This precluded the automated determination of SWE from the Kinar and Pomeroy (2007) technique. The implications are that acoustic sampling of SWE could not be efficiently performed at the same time scale as other measurements taken at a meteorological station due to the large amounts of data that must be interpreted. Moreover, use of this acoustic technique for snow surveying did not permit the surveyor to immediately determine whether the acoustic measurement was successful and adapt the field measurement design to measurement success.

This paper outlines how the theory and signal processing of the Kinar and Pomeroy (2007) acoustic technique have been recently improved so that they can be used in an operational context. This permitted the signal processing to be conducted in the field using custom electronic circuits that are portable and easily transported to remote locations. The device constructed for signal processing allowed for repeatable measurements of SWE to be made using an acoustic wave. Because the electronics had to be designed in a particular fashion to perform acoustic sampling of SWE, the attenuation of sound by snow and the effect of frequency on the propagation of the sound wave in the snowpack were also investigated. These measurements contribute to observations made by other investigators in snow acoustics and help to establish observational techniques for further research into the physical properties of snow.

THEORY

The physical system of the snowpack is considered to be the same as described by Kinar and Pomeroy (2007). The snowpack consists of a layered, porous medium. The "layers" are acoustic layers, due to observable changes in the acoustic properties of snow. A sound pressure wave is created in the air above the snow surface by a downward-facing transducer. As predicted by the Biot theory of sound propagation through porous media (Biot, 1956a, Biot 1956b), the sound pressure wave propagates in the pore spaces of the snowpack (Johnson, 1982) as two types of pressure wave (P_1-wave and P_2-wave) and one type of shear wave (S-wave). The P_1-wave travels through the ice matrix, whereas the P_2-wave propagates through the pore spaces of the snowpack. The S-wave propagates through the ice matrix. Movement of these three types of waves is coupled. This application is concerned with the P_2-wave propagating through the pore spaces of the medium, which are assumed to air-filled.

Given the reflection coefficient Γ_k, the porosity of layers L_1 and L_k in the snowpack can be determined by recursive calculation (Kinar and Pomeroy, 2007):

$$\phi_1 = \alpha_1^{1/2}\left[\frac{1-\Gamma_1}{1+\Gamma_1}\right] \tag{1}$$

$$\phi_k = \frac{\alpha_k^{1/2}}{\alpha_{k+1}^{1/2}}\left[\frac{1-\Gamma_k}{1+\Gamma_k}\right] \tag{2}$$

Equation 1 and 2 involve two unknown parameters $\{\alpha,\phi\}$, where the tortuosity of the snow is α and the porosity is ϕ. The tortuosity is a bulk geometric parameter which can be defined as the deviation of the straight-line distance through the pore spaces of a medium, and the porosity is a measurement of the fraction of pore spaces in snow. If one of the parameters in the set $\{\alpha,\phi\}$ is known, the other parameter can be determined. A relationship between the tortuosity and the porosity of porous materials has been identified from Biot theory by Berryman (1980), who found that a relationship between the porosity and the tortuosity of a porous medium is dependent on a shape factor γ determined from the geometry of the particles that comprise the medium:

$$\alpha_k = 1-\gamma(1-\phi) \tag{3}$$

The shape factor γ ranges between $0.5 \le \gamma \le 0.67$ (Berryman, 1980, 1983; Johnson and Sen, 1981). This factor is from the expression $m = \gamma\rho_0$, which is used in Biot theory to represent the mass m induced by movement of the particles comprising the porous frame saturated with a fluid of density ρ_0 (kg m^{-3}).

Suppose that γ is unknown, and that a simplification of Equation 3 is necessary. If the frame is assumed to be completely rigid for snow, the induced mass could be taken as $m \approx 0$. In the context of Biot theory, this would also assume that the P_2 and S waves would not propagate in the porous medium, although it has been postulated that shear waves may actually be produced due to interactions between the grains comprising the porous media frame (Buckingham, 2000). Returning to the derivation presented by (Berryman, 1980) of Equation 3, this expression for the tortuosity is exactly equal to unity ($\alpha_k = 1$) when $m = 0$. This would imply that the boundary conditions at the air-snow and snow-snow interfaces are similar, and Equations 1 and 2 would be identical. Such an assumption is not physically reasonable and would strongly suggest that the tortuosity of snow cannot be considered as exactly equal to unity. In lieu of any further information, we approximate the shape factor as $\gamma = 0.59$, which is in the middle of the range.

The sound pressure wave interacts in a complex fashion with the "layers" of the snowpack due to internal reflections and attenuation. To model this behaviour, the snowpack can be considered as a digital filter which acts on the frequency-swept wave $s(t)$ from the transducer sending the sound pulse into the snow. Assuming that the reflection coefficients are given by $r(t)$ and that the attenuation of the snowpack is $a(t)$, the overall sound pressure wave reflection $s'(t)$ from the snowpack can be modeled as the convolution:

$$s'(t) = \int_{-\infty}^{+\infty}\int_{-\infty}^{+\infty} s(\tau)\,r(t-\tau)\,d\tau\,a(\tau)\,d\tau = s(t) * r(t) * a(t) \tag{4}$$

The reflection $s'(t)$ that reaches the receiving transducer will be the P_2-wave travelling back across the snow-air boundary. Although the P_1-wave and S-wave will also propagate in the snow, the P_1-wave will have small amplitude due to the stiffness of the frame, and because the S-wave exhibits shear motion, it will not be detected in the air medium for small angles of θ because the air is incapable of shear motion. Digital signal processing is then used to determine the reflection coefficients at each of the layers.

SIGNAL PROCESSING

The reflection $s'(t)$ from the snowpack is detected by the receiving transducer as a dual-polarity analog voltage proportional to the sound pressure incident on the sensing element. The voltage from the transducer is digitized using an Analog-to-Digital Converter (ADC) which samples at a frequency $f_c > 2f_i$ greater than Nyquist to ensure that aliasing does not occur. The output of the ADC is a time series of voltage measurements which is then normalized to the interval $[-1.0,1.0]$ using the highest voltage that can be quantized. The continuous function $s'(t)$ can be re-written as a discrete function $s[t]$ which also includes the effects of the sampling system:

$$s'[t] = \left\{ r[t] * \left(s[t] * s_t[t] * a[t] \right) * s_r[t] + n_m[t] + n_s[t] + n_e[t] + n_w[t] \right\} \tag{5}$$

where $r[t]$ is the reflection response of the snowpack, $s[t]$ is the original frequency-swept wave that is produced, $s_t[t]$ is the frequency response of the sending transducer which is assumed to not be linear over the time that the frequency-swept wave is produced, $a[t]$ is the attenuation function of the snowpack which models the reduction in amplitude of the P_2-wave travelling through the snow medium, $s_r[t]$ is the time-domain response of the transducer which receives the wave, $n_m[t]$ is the air-coupled direct wave that travels in the air between the sending and receiving transducers, $n_s[t]$ is the noise produced by the sampling system, $n_e[t]$ is environmental sources of noise, and $n_w[t]$ is a function that includes wind effects that act on the receiving transducer. Because $n_s[t] + n_e[t]$ cannot be directly measured, $n_s[t]$ is attenuated by a matched filtering algorithm which increases the Signal-to-Noise Ratio (SNR) by the addition of white noise.

The contribution of the air-coupled direct wave $n_m[t]$ is difficult to predict because the sensing system consists of only one receiving transducer. Another transducer could be positioned between the sending transducer and the receiving transducer, but sampling of the pressure wave in this fashion requires an additional electronic circuit and also increases the processing time. Moreover, the presence of another transducer may affect the spatial sound pressure distribution of the direct air-coupled wave, and the estimation of $n_m[t]$ would be inaccurate. To remove $n_m[t]$, the contribution of the air-coupled wave to $s'[t]$ is considered to be similar to crosstalk between two wires. Crosstalk occurs in electronics when a signal produced in one channel of a data system leaks over to another channel, creating an unwanted signal. Removal of $n_m[t]$ utilizes the minimization of a δ coefficient (Claerbout, 1992):

$$\delta = \min \left[\sum_{i=1}^{N} \frac{\left\{ s''[t] - \delta \left(s[t] * s_t[t] \right) \right\}^2}{\left(s[t] * s_t[t] \right)^2 + \sigma^2} \right] \tag{6}$$

where σ is the median of the voltage levels in the signal $s[t] * s_t[t]$.

Once the δ coefficient has been found by minimization, the air-coupled wave is calculated as $n_m[t] = \delta s[t]$ and subtracted from $s'[t]$, resulting in the expression:

$$s'''[t] = r[t] * \left(s[t] * s_t[t] * a[t] \right) * s_r[t] \tag{7}$$

The sound pressure wave $s[t]*s_t[t]$ produced by the transmitting transducer is modeled by first generating a signal $s[t]$ frequency-swept between two frequencies f_0 and f_1, and then convolving the generated signal $s[t]$ with the time-domain response of the transducer:

$$s[t]=\sin\left(2\pi\left\{f_0+\frac{f_1-f_0}{2\Delta t}t\right\}\right) \tag{8}$$

$$s[t]*s_t[t]\Leftrightarrow s[f]s_t[f] \tag{9}$$

where $\Delta t=t_1-t_0$ is the time duration of the sweep, $s[f]$ is the frequency-domain version of the signal sent from the transducer, and $s_t[f]$ is the frequency response of the transmitting transducer. The conversion between the time and frequency domains is performed by the Fast Fourier Transform (FFT), which can be easily implemented on most digital signal processors (DSPs). Because convolution in the time domain is equivalent to multiplication in the frequency domain, the transmitting sensor response $s[t]*s_t[t]$ is calculated by separately applying the FFT to $s[t]$ and $s_t[t]$, multiplying $s[f]$ and $s_t[f]$ in the frequency domain and then converting $s[f]s_t[f]$ back into the time domain by the Inverse Fast Fourier Transform (IFFT). Because the frequency domain signals $s[f]$ and $s_t[f]$ are comprised of real and imaginary parts, this is a multiplication of complex numbers. Following (Brittle et al., 2001), the conversion between time and frequency domains is then used to obtain the reflection response from the snowpack:

$$r[t]*a[t]\Leftrightarrow\frac{s'''[f]}{s[f]*s_t[f]*s_r[f]} \tag{10}$$

where $s[f]*s_t[f]*s_r[f]\neq 0$ over the frequency domain of interest since the transmitted sweep $s[f]$ and the frequency response of the transducers $s_t[f]$ and $s_r[f]$ are non-zero. This is reasonable if the operating ranges of the transducers are selected for the frequency range of interest and $s[f]$ will always be non-zero.

Although it is possible to obtain reflection coefficients using techniques adapted from seismology (Kinar and Pomeroy, 2007), there is a simpler processing technique which uses theory taken from radar applications. This reduces the number of software loop iterations required to implement seismic methods of deconvolution, speeds up the execution time of the processing algorithm and also eliminates the need for assumptions to be made concerning the statistical properties of the reflection response.

The FMCW signal processing is implemented by homodyning (mixing) the reflection response $r[t]*a[t]$ with the frequency sweep $s[t]$. Performed in the time domain, the mixing operation is implemented digitally by multiplying $r[t]*a[t]$ with $s[t]$ using point-by-point multiplication to produce the signal $h[t]$. The signal is then taken into the frequency domain by the FFT. Characteristic of $h[f]$ is the presence of peaks that occur at beat frequencies $f_{b,k}$. Each peak represents an interface Ω_k between two layers of the snowpack which can be scaled to find the reflection coefficients between the layers (Deng and Liu, 1999).

A layer-stripping approach (Deng and Liu, 1999) adapted from radar theory is used to recursively relate the reflection coefficients $\{\Gamma_1,\ldots,\Gamma_N\}$ of the sound pressure wave to the amplitudes $\{A_1,\ldots,A_N\}$:

$$A_k = \begin{cases} \Gamma_0 & \text{for } k = 0 \\ \Gamma_k \prod_{i=1}^{k} (1 - \Gamma_i) & \text{for } k > 0 \end{cases} \tag{11}$$

Because A_k is the normalized amplitude on the scale $[-1,1]$, the relationship of the receiving transducer T_r to the SPL of the reflected wave is (Raichel, 2006):

$$E_k = \zeta \left(2 \times 10^{-4}\right) 10^{(L+L_r)/20} \tag{12}$$

where L is the SPL of the wave at the surface of the transducer, L_r is the sensitivity of the transducer (in dB and referenced to a level of $1\ \mathrm{V}/\mu\mathrm{bar}$), and $\zeta \in \mathbb{R}$ is used to normalize the voltage to the same scale as the A_k.

From the beat frequency spectrum calculated by homodyning, the distance from the sending transducer T_s to the surface of the snowpack is given by (Yankielun et al., 2004; Kinar and Pomeroy, 2007):

$$y_0 = \frac{f_{b,1} \Delta t c_0}{2B} \tag{13}$$

where $f_{b,1}$ (Hz) is the beat frequency of the first "peak" in the beat frequency spectrum, Δt is the time of the sweep, $B = f_1 - f_0$ is the bandwidth of the sweep, with f_0 (Hz) and f_1 (Hz) being the starting and ending frequencies of the sweep, $c_0 = \left(1.4RT^*\right)^{1/2}$ is the phase velocity of sound in air (m s^{-1}), R is the thermodynamic gas constant of air (N m kg^{-1} K^{-1}), and T^* is the average temperature of the air above the snow surface (K). Although it is possible for strong temperature gradients to develop above the surface of the snowpack, the temperature T^* is taken to be the average temperature in lieu of any other measurements.

To determine the reflection coefficients at the snowpack interfaces, the transducer radiating the sound wave is modeled as a piston that vibrates in the half-space above the snow surface (i.e. Kinsler and Fry, 1962). The transmitted pressure wave p_0^t across the air-snow interface Ω_0 is then calculated from the sonar equation, the definition of the Sound Pressure Level (SPL, the pressure of the acoustic wave at the interface expressed in decibels), and the continuity relationship of the reflected, incident, and transmitted waves at the boundary:

$$L_0 = L_s - 20 \log\left(\frac{ak^2}{4y_0 \sin\left(0.5ak\right)}\right) \tag{14}$$

$$p_0^+ = p_{ref} 10^{L_0/20} \tag{15}$$

$$p_0^t = p_0^+ \left(1 + \Gamma_0\right) \tag{16}$$

where $p_{ref} = 2.0 \times 10^{-5}$ Pa is the reference pressure (Pa), p_0^+ is the sound pressure of the wave incident on the snow surface (Pa), L_0 is the SPL of the wave at the first interface in decibels, the reflection coefficient is Γ_0 (dimensionless), the radius of the transducer is a (meters), the wavenumber is k (m^{-1}), the distance to the first interface is y_0 (meters),

The attenuation coefficient ψ_k for a layer L_k of dimension y_k (meters) is calculated from (Meyer and Newman, 1972):

$$\psi_k = \frac{\partial p}{\partial y}\frac{1}{2\overline{c}_k \rho_0 c_0^2} \tag{17}$$

where $\partial p / \partial y$ is the pressure gradient (Pa m^{-1}) established in the layer L_k. Assuming that the pressure gradient between the interfaces Ω_k and Ω_{k+1} of the snowpack is linear and that the decay rate of the pressure wave in the porous medium is exponential, an expression for the attenuation in the layer is given by:

$$\psi_k = \frac{p_k^t e^{-\psi_k y_k} - p_k^t}{2 y_k \overline{c}_k \rho_0 c_0^2} \tag{18}$$

where y_k is the distance to a layer (meters), the transmitted pressure wave across the interface is p_k^t (Pa), the phase velocity of the wave in the layer is $\overline{c}_k$ (m s^{-1}), the density of the air medium is ρ_0 (kg m^{-3}), and the phase velocity of the sound pressure wave in air is c_0 (m s^{-1}).

The distance to each of the layers of the snowpack is found by modifying Equation 13 to account for multiple reflectors (Kinar and Pomeroy, 2007):

$$y_k = \frac{\overline{c}_k}{2B}\left(\Delta f_{b.k}\Delta t - 2B\sum_{i=1}^{k-1}\frac{y_i}{\overline{c}_i}\right) \tag{19}$$

where $\Delta f_{b.k}$ (Hz) is the beat frequency at each successive "peak" in the homodyned beat frequency spectrum.

The variables $\{a_k, \overline{c}_k, y_k, \phi_k, \alpha_k\}$ are determined in a recursive fashion using versions of Equations 19, 18, 16, 15, 14, 13, 10, 1, and 2, adapted for successive "layers" in the snowpack. The density of the snow is calculated from the expression:

$$\rho_k = \rho_{\text{ice}}\left(1 - \phi_k\right) \tag{20}$$

where $\rho_{\text{ice}} = 917$ kg m^{-3}. Assuming that 1 kg of water has a depth of 1 mm over an area of 1 m^2, the depth-integrated SWE is then calculated from the depth and density of each of the layers (Pomeroy and Gray, 1995):

$$\text{SWE} = \frac{Y}{N}\sum_{i=0}^{N}\rho_i \tag{21}$$

EXPERIMENTAL SETUP

Two prototype devices were constructed to collect acoustic SWE data (Figure 1 and Figure 2). Both prototypes used custom circuit boards which were designed in-house at the University of Saskatchewan Centre for Hydrology. Each system was comprised of a 32-bit Digital Signal Processor (DSP) running at a frequency in the MHz range. Both systems were designed with 8 MB of flash memory and over 200 MB of volatile Random-Access Memory (RAM) for temporary storage of data during gauge operation. The memories were interfaced to the DSP over a high-speed data bus without external glue logic. The Linux™ operating system was installed on the flash memory of the gauge, and the open-source U-BOOT bootloader was used to set up the DSP and load the Linux kernel into RAM. The startup routine of the DSP took less than five seconds.

The frequency-swept sound wave was produced by a specialized Digital-to-Analog Converter (DAC) which created a frequency-swept signal. The signal was amplified by an audio amplifier and converted into an audible sound by a transmitting transducer. For the first prototype deployed during the winter of 2007, the sound pressure wave produced by the transmitting transducer was frequency-swept between 20 Hz and 20 kHz. The duration of the wave was ~1

second, and all frequencies produced were in the audible sound range. Although it was not possible to completely reproduce all of the frequencies in this range due to the finite frequency response of the transmitting transducer, the frequency response of the transducer obtained from a datasheet was used in the de-convolution process (Equation 10). Alternately, the second prototype used a frequency-swept wave which was linear over a small range of frequencies. In a similar fashion to frequency-swept techniques in seismology, this was an attempt to reduce attenuation of the sound pressure wave as it travelled in the snow.

Figure 1: First prototype snow sonar device being deployed at the Yukon sites.

Figure 2: Second prototype snow sonar device deployed at the Rocky Mountain sites.

The reflected signal from the snowpack was detected by a transducer, and the produced voltage signal was amplified by an operational amplifier and digitized by a 24-bit ADC. Power supplies to this sensitive ADC were filtered to prevent noise from contaminating the input signal. The digitized signal was then subjected to processing by the DSP, which ran a program implementing the mathematics described in this paper.

Because the first prototype of the snow sonar device was an earlier version of the second prototype device, peak detection had to be performed off-line before the algorithms were finalized. The final version of the algorithm was deployed in the second prototype version of the gauge.

Estimates of average depth, density, and SWE of the snowpack were displayed on an LCD display attached to the front of the gauge so that the operator could evaluate the measurement. The program used to process the data took less than three seconds to fully process the reflected signal from the snowpack. This was an improvement over the signal processing described in the paper by Kinar and Pomeroy (2007), which used seismic deconvolution algorithms that are better suited for off-line signal processing.

Both gauges were equipped with a trigger grip and a push-button. The gauge operator could press the push-button to initiate a sampling measurement. A keypad situated on the top of the device could be used to enter additional information. Data from the gauge was written down in a field notebook or stored in the internal flash memory for additional off-line processing. A Universal Serial Bus (USB) connection was used to offload data to a computer.

FIELD LOCATIONS

The acoustic instruments were tested at two field sites. The first prototype was tested during the late winter of 2007 in Wolf Creek Research Basin, near Whitehorse, Yukon Territory, whereas the second device was tested during the winter of 2008 at field locations in the Rocky Mountains, Alberta, Canada.

Wolf Creek, Yukon Territory

Wolf Creek Research Basin is a mountainous catchment located near to Whitehorse, Yukon. Vegetation cover is primarily shrub tundra, alpine tundra and boreal forest (Granger, 1999). The first prototype of the acoustic gauge was tested during April 2007 in the valley bottom of Granger Basin (GB), a sub-catchment situated within the Wolf Creek Basin. The vegetation at this site was representative of shrub tundra composed of willow and birch from 30 cm to 2 m tall. Snow at GB was heavily crusted by wind and melt but was cold and dry with extensive depth hoar formation Additional tests were also conducted under the canopy of a discontinuous white spruce stand in the boreal forest (BF) at lower elevations in Wolf Creek Basin.

Rocky Mountains, Alberta

The second prototype of the acoustic gauge was tested during May 2008 in the Spray River valley east of Banff National Park. The first test site was situated less than one km from the Burstall Pass trail parking lot. Testing was conducted in an open area near a sub-alpine forest (BP-open) and on a ridge (BP-ridge) near the parking lot. BP-open snow was melting with air temperatures near 7^{o} C during sampling. BP-ridge snow had undergone melt but was cold and relatively dry during sampling. The Mount Shark sampling locations (MS) were situated near the Mount Shark parking lot in an area interspersed with sparse fir (*Abies* sp.) and spruce (*Picea* sp.) trees. Snow here was similar to the BP-ridge snow.

PROCEDURE

Yukon Sites

Eight sampling locations were selected along a transect in the valley bottom of Granger Basin (GB). At each sampling point, the acoustic device was pointed at the snow surface and an acoustic measurement of SWE was initiated by pressing the trigger button. After the acoustic SWE sample was collected, a snowpit was dug directly under the measurement point. Layers were identified by examination of hardness and crystal habit. The density of each layer in the snowpit was obtained by gravimetric sampling using a triangular snow sampler. The snowpit stratigraphy was recorded. Observations were also made of the presence of vegetation trapped

beneath the snow surface. Many samples had willow shrubs buried under the measurement site. A hard wind crust was observed on the top of the snowpack, and ice layers were scattered throughout the snowpack.

This acoustic sampling technique was repeated under the boreal forest canopy (BF). Due to the presence of trapped vegetation and forest detritus beneath the snow surface, it was not possible to dig a snowpit at all of the sampling locations. Fourteen sampling locations were identified. An acoustic measurement of SWE was taken before disturbing the snow surface. At these locations, SWE was estimated using a snowpit and an ESC30 snow sampler.

Rocky Mountain Sites

At the Burstall Pass test site (BP-open) before the snow surface was disrupted, the snow sonar device was used to take samples at five points. Snowpits were dug at each of the points, and gravimetric samples were taken from each of the layers identified. Snowpit stratigraphy was also recorded. Gravimetric SWE measurements with an ESC30 snow sampler were also taken. Because the sampling procedure occurred during the morning and mid-afternoon, the snowpack was slightly wetted at the surface but generally dry at depth.

A second transect was set up along a ridge overlooking the Burstall Pass parking lot (BP-ridge). Acoustic sampling with the snow sonar device was conducted at 13 sampling points situated in the open and in close proximity to shallow snow near large coniferous trees. Immediately after using the snow sonar device, gravimetric samples of SWE were taken with an ESC30 snow sampler. Because the sampling occurred during the morning, the snowpack was refrozen and dry.

Sampling in the Mount Shark area occurred along a transect situated between the trees (MS). The acoustic gauge was used to sample in the vicinity of tree wells and in the open, unsheltered areas. Gravimetric measurements of SWE were taken with an ESC30 snow sampler at each of the acoustic sampling points. The snowpack was observed to be dry, and the snow surface was hard and icy. All measurements were completed before the surface of the snowpack started to become wet.

ANALYSIS AND RESULTS

For most sampling points, the algorithm used to determine SWE found the reflection coefficients of the sound pressure wave from the layered interfaces in the snowpack. An example output of this calculation is shown as Figure 3. The automated peak detector used to locate the reflections from the layers was able to determine the position of each peak and obtain an estimate of the beat frequency used in the calculation of Equation 5. However, the peak detector was often unable to identify the reflection from the bottom of the snowpack due to reverberation effects when the wave encountered multiple reflections from the snow and attenuation of the sound pressure wave. This necessitated an estimate of the maximum snow depth. For the first prototype gauge, the depth estimate was used when the reflected wave from the snow was subjected to off-line signal processing. When the second prototype gauge was developed, the depth estimate (from a ruler) was entered using the keypad of the gauge before the acoustic sample was taken. This permitted the peak detector to operate immediately after the acoustic measurement had been initiated by the push-button switch. In most cases, the reflection coefficients did not spatially correspond with observable layers in the snowpack. Reflections occurred due to changes in the acoustic properties of the snow, which did not always correspond with classical snowpack stratigraphy. Results from the various sites are listed in Table 1.

Results from the Granger Basin site (GB, Figure 4) show that there was an average difference of 27% (Mean Error = 40 mm, $R^2 = 0.71$) between the gravimetric and sonar estimates of SWE. Sampling points 2, 6, and 9 demonstrate the effects of buried shrubs on the output of the acoustic device. The acoustic SWE can be underpredicted (sampling points 2 and 6) or overpredicted due to scattering of the sound wave by the buried vegetation. Because very thick wind crusts and ice layers were observed in snowpack stratigraphy, the Granger Basin site suggests that the acoustic technique can still perform reasonably well for snow that has

accumulated in a complex fashion on natural landscapes. It should be noted that dense shrubs precluded use of the ESC30 snow tube in these GB sites – the tube became trapped in the vegetation and disturbed the snowpack.

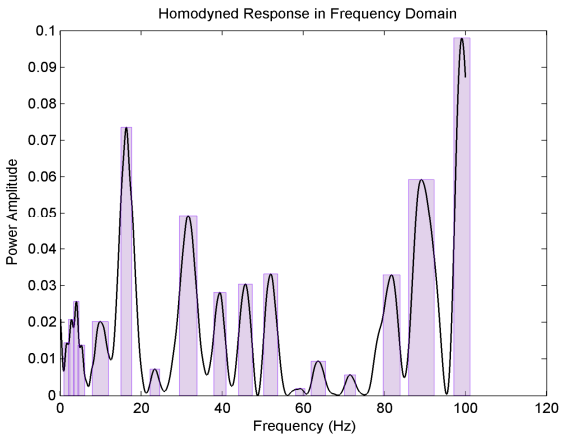

Figure 3: Output of the peak detector used to identify reflections from the snow.

Table 1. Results from field sites

Location	Comparison	Error (%)	Mean Error (mm)	R^2 Correlation
Granger Basin GB	Snowpit & Sonar	27	40	0.71
Boreal Forest BF	Snowpit & Sonar	12	16	0.52
Boreal Forest BF	ESC30 & Sonar	26	38	0.57
Boreal Forest BF	ESC30 & Snowpit	14	31	0.81
Burstall Pass BP-open	Snowpit & Sonar	6	25	0.60
Burstall Pass BP-open	ESC30 & Sonar	36	111	0.38
Burstall Pass BP-open	ESC30 & Snowpit	19	77	0.33
Burstall Pass BP-ridge	ESC30 & Sonar	10	21	0.72
Mount Shark MS	ESC30 & Sonar	20	23	0.79

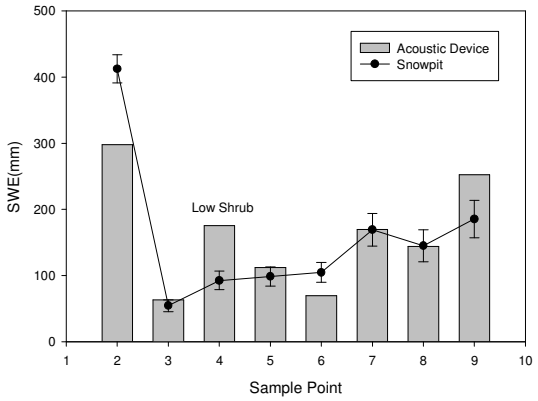

Figure 4: Comparing measured and acoustic estimates of SWE from the Yukon Granger basin site (GB).

The boreal forest site in the Yukon (BF) also shows the effects of vegetation on the acoustic SWE technique. Owing to buried logs, small trees, detritus from the forest canopy and hard snow layers, scattering of the sound wave was so pronounced that acoustic estimates of SWE could not be obtained for some points due to the absence of a reflected wave that should have been detected by the snow sonar device. These missing data points (Figure 5) occurred at positions

along the transect where logs were embedded under the snow surface. Buried twigs and branches were responsible for the variation observed at the other sampling points. The overall difference between the ESC30 and snowpit estimates of SWE was 14% (Mean Error = 31 mm, R^2 = 0.81). The difference between the ESC30 and acoustic estimates of SWE was 26% (Mean Error = 38 mm, R^2 = 0.57, whereas the difference between the snowpit and acoustic estimates was 12% (Mean Error = 16 mm, R^2 = 0.52). These results demonstrate that the error between acoustic and snowpit measurements of SWE is less than the error between ESC30 and snowpit estimates.

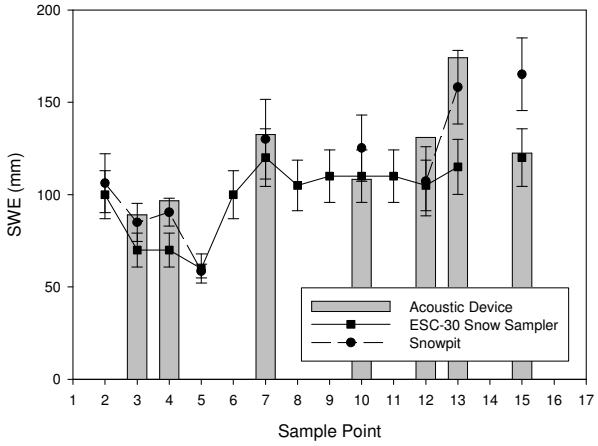

Figure 5: Comparing measured and acoustic estimates of SWE from the Yukon boreal forest site (BF).

The data collected at the Rocky Mountain Burstall pass site (BP-open) demonstrated the effects of wet, melting snow on the acoustic technique (Figure 6). The average difference between the ESC30 and snowpit SWE was 19% (Mean Error = 77 mm, R^2 = 0.33), which is 5% higher than the difference in SWE observed between these two types of observations at the boreal forest site (BF) in the Wolf Creek basin and suggests problems with ESC30 measurements under these conditions. The average percentage difference between the snowpit and sonar measurements of SWE was smaller at 6% (Mean Error = 25 mm, R^2 = 0.60), which was lower than the percentage differences between these two measurements at the Wolf Creek sites and similar to the differences observed at the BP-ridge site. The difference between the ESC30 snow sampler and the acoustic technique was 36% (Mean Error = 111 mm, R^2 = 0.38). Although the Biot (1956a, 1956b) theory model cannot be used for wet snow because the pore spaces of the snowpack have a mixture of air and water, and the assumption of this model applied to snow is that the pore spaces are only saturated with one type of fluid (air), the results show that the acoustic technique can still produce estimates of SWE that are accurate. Smaller percentage differences occured between snowpit and sonar measurements of SWE as compared to ESC30 and snowpit measurements, suggesting superior performance of the acoustic measurement over the snowtube if one assumes that the snowpit is the most reliable observation method.

In contrast, the SWE transect situated on the ridge near the Burstall Pass parking lot (BP-ridge) had low differences between the ESC30 and sonar SWE estimates (Figure 7). The overall percentage difference between the two methods was only 10% (Mean Error = 21 mm, R^2 = 0.72). Higher SWE estimate differences occurred when samples were taken in close proximity to tree wells. Sonar SWE differences could have been underpredicted (sample point 7) and overpredicted (sample point 6) due to lateral propagation of the sound pressure wave though the side of the tree well formation and into the air surrounding the trunk of the tree. ESC30 density measurements may also have had greater error near trees due to clumps of buried unloaded intercepted snow which can interfere with collection of a snow core.

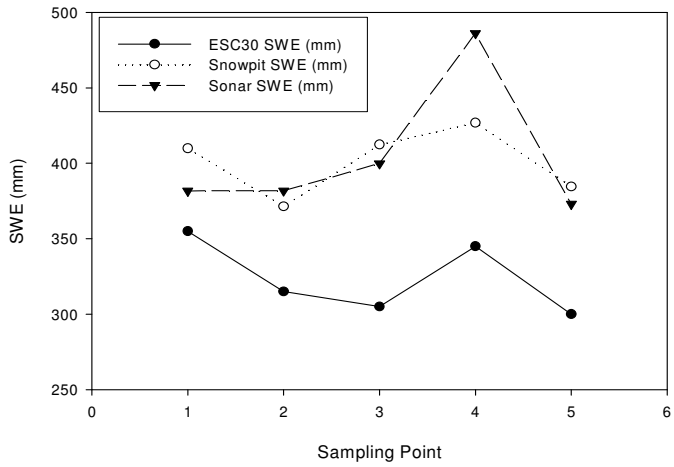

Figure 6: Comparing gravimetric and acoustic estimates of SWE from the Burstall Pass Site

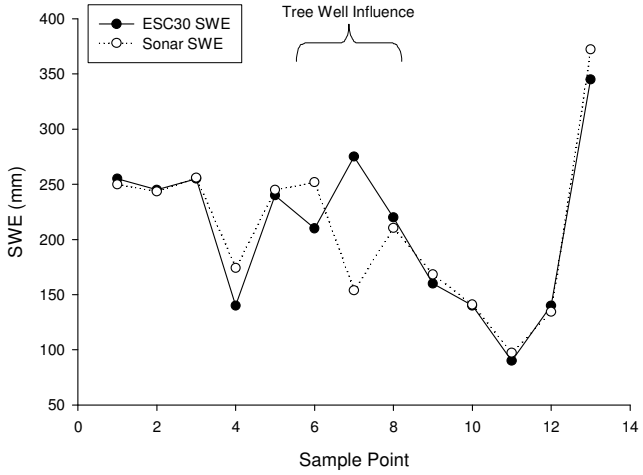

Figure 7: Comparing gravimetric and acoustic estimates of SWE from the Burstall Pass transect (BP-ridge)

For the Mount Shark survey (Figure 8), the percentage difference between the ESC30 and acoustic SWE measurements was 20% (Mean Error = 23 mm, R^2 = 0.79). This difference is greater than the difference between estimates for the transect performed on the ridge near the Burstall pass parking lot (BP-ridge) and greater than the differences between ESC30 and sonar estimates at the Burstall pass site (BP-open). The percentage difference is comparable to the difference between estimates observed at the Granger Basin site (GB). The Mount Shark survey (MS) is particularly encouraging since the SWE determined by gravimetric sampling with the ESC30 and the acoustic estimates of SWE from the model presented in this paper show a strong correlation along the length of the transect, and consequently, the plots of both observations have a similar form.

CONCLUSIONS

The results of experiments at a mixture of forested and open sites in two geographically-distinct regions over two winter field seasons demonstrated that for cold, dry snow, an acoustic wave can determine SWE with accuracy comparable to the differences between gravimetric sampling by snowpit and ESC30 snowtube. Although the acoustic model of sound propagation used in this paper assumes that the pore spaces of snow are completely air-filed, the results

demonstrate that similar estimates of SWE are still obtained when the snowpack is wetted. The acoustic results have a higher accuracy when compared to estimates of SWE from snowpit measurements rather than a snowtube because the layered gravimetric sampling allows for a depth-integrated estimate of the density and is therefore a more accurate estimator of SWE than the bulk estimate from the ESC30 gauge. Further research is required to develop a model that is able to incorporate the effects of snowpack wetness in the equations used to determine SWE. Testing of this new model would require quantitative estimates of snow wetness, which can be obtained by dielectric and capacitance observations.

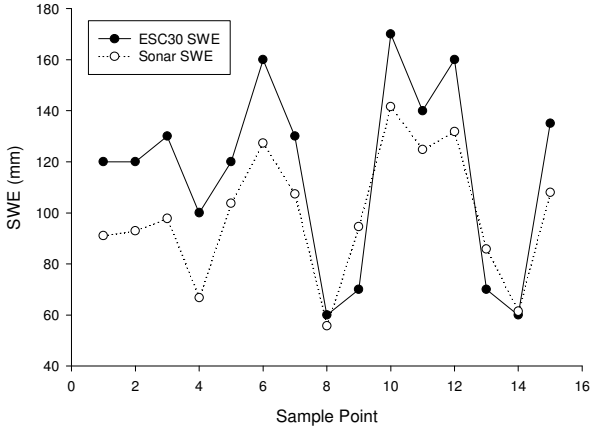

Figure 8: Comparing measured and acoustic estimates of SWE from the Mount Shark Survey (MS)

Further research is also required to mathematically model the interactions of the sound wave with ice layers and vegetation. Prediction of sound wave scattering by buried vegetation may help to provide insights into mitigating this effect and improving the acoustic estimates of SWE.

The use of a fixed shape factor $\gamma = 0.59$ allows for SWE to be adequately predicted by an acoustic wave at two field sites. This suggests that this value is adequate for most operational deployments of the snow sonar gauge, but setting shape factors to local conditions might improve gauge performance.

This paper demonstrates that SWE can be determined using acoustic waves in an automated fashion, controlled and calculated on site using electronic circuitry. It is possible that this technique can prove to be valuable to snow surveyors, who currently have to extract snow samples from the snowpack to determine SWE. The use of a non-invasive method has the potential to revolutionize snow surveying and permit snow samples to be taken much more quickly than with a snow tube or snowpit. This allows for snow surveyors to perform their task quickly and allows for a greater number of sampling points to be collected along a transect. Other potential applications for the snow sonar gauge include automated determination of SWE at a fixed site in remote locations and the examination of high-resolution temporal changes in the snowpack. Further research is planned to verify the conclusions presented in this paper and assess the feasibility of these other novel applications of the technology.

ACKNOWLEDGEMENTS

We would like to thank Warren Helgason and Pablo Dornes (University of Saskatchewan) and Rick Janowicz (Yukon Environment) for logistical assistance at the Wolf Creek sites, and Anne Sabourin (L'Ecole Polytechnique Paris, France), Richard Essery (University of Edinburgh, Scotland) and the University of Calgary Biogeoscience Institute for assistance with the field campaign conducted in the Rocky Mountains. This research was funded by the International Polar Year (IPY), the Canadian Foundation for Climate and Atmospheric Sciences (CFCAS) through a grant to the IP3 Network, an NSERC scholarship and by the Canada Research Chairs Program.

REFERENCES

Barrande, M, Bouchet, R, and Denoyel, R. 2007. Tortuosity of porous particles. *Analytical Chemistry* **79**: 9115-9121.

Berryman, JG. 1980. Confirmation of Biot's Theory. *Applied Physics Letters* **37**: 382-384.

Berryman, JG. 1983. Effective conductivity by fluid analogy for a porous insulator filled with a conductor. *Physical Review B* **27**: 7789-7792.

Biot, MA. 1956a. Theory of propagation of elastic waves in a fluid-saturated porous solid. I . Low frequency range. *Journal of the Acoustical Society of America* **28**: 168-178.

Biot, MA. 1956b. Theory of propagation of elastic waves in a fluid-saturated porous solid. II. Higher frequency range. *Journal of the Acoustical Society of America* **28**: 179-191.

Brittle, K, Lines, LR., and Dey, AK. 2001. Vibroseis deconvolution: a comparison of cross-correlation and frequency-domain sweep deconvolution. *Geophysical Prospecting* **49**: 675-686.

Buckingham, MJ. 2000. Wave propagtion, stress relaxation, and grain-to-grain shearing in saturated, unconsolidated marine sediments. *Journal of the Acoustical Society of America* **108**: 2796-2815.

Claerbout, JF. 1992. *Earth Soundings Analysis: Processing versus Inversion*. Cambridge, Massachusetts: Blackwell Scientific Publications.

Deng, R, and Liu, C. 1999. FM-CW radar performance in a lossy layered medium. *Journal of Applied Geophysics* **42**:23-33.

Granger, RJ. 1999. Partitioning of energy during the snow-free season at the Wolf Creek Research Basin *in* J. W. Pomeroy, and Granger, R.J., editors. Wolf Creek Research Basin: Hydrology, Ecology, Environment, Proceedings of a Workshop held in Whitehorse, Yukon, 5-7 March 1998. National Water Research Institute, Saskatoon, Saskatchewan.

Johnson, DL., and Sen, PN. 1981. Multiple scattering of acoustic waves with application to index of refraction of fourth sound. *Physical Review B* **24**:2486-2496.

Johnson, JB. 1982. On the application of Biot's theory to acoustic wave propagation in snow. *Cold Regions Science and Technology* **6**:49-60.

Kinar, NJ., and Pomeroy, JW. 2007. Determining snow water equivalent by acoustic sounding. *Hydrological Processes* **21**:2623-2640.

Kinsler, LE., and Fry, AR. 1962. *Fundamentals of Acoustics*. New York; London; Sydney: John Wiley & Sons.

Male, DM., and Gray, DH. 1975. Problems in developing a physically-based snowmelt model. *Canadian Journal of Civil Engineering* **2**:474-488.

Meyer, E, and Newman, EG. 1972. *Physical and Applied Acoustics: An Introduction*. New York and London: Academic Press.

Pomeroy, JW., and Gray, DM. 1995. *Snowcover: Accumulation, Relocation, and Management*. National Hydrology Research Institute Science Report No. 7,. National Water Research Institute, Saskatoon.

Pomeroy, JW., Hedstrom, N, and Parviainen, J. 1999. The snow mass balance of Wolf Creek, Yukon: Effects of snow sublimation and redistribution. Pages 15-30 *in* J. W. Pomeroy, and Granger, R.J., editor. Wolf Creek Research Basin: Hydrology, Ecology, Environment, Proceedings of a Workshop held in Whitehorse, Yukon, 5-7 March 1998. National Water Research Institute, Saskatoon, Saskatchewan.

Pomeroy, JW, Gray, DM, Brown, T, Hedstrom, NR., Quinton, WL., Granger, RJ., and Carey, SK. 2007. The cold regions hydrological model: a platform for basing process representation and model structure on physical evidence. *Hydrological Processes* **21**: 2650–2667.

Raichel, D. R. 2006. The *Science and Applications of Acoustics, Second Edition*. New York: Springer.

Yankielun, N. 1992. Alpine snow depth measurements for aerial FMCW radar. *Cold Regions Science and Technology* **40**:123-134.